Nanoscale eluting coatings based on alginate/chitosan hydrogels

Ping Peng[a)]
Ian Wark Research Institute, University of South Australia, Mawson Lakes, Adelaide,
South Australia 5095, Australia

Nicolas H. Voelcker
School of Chemistry, Physics and Earth Sciences, Flinders University, GPO Box 2100,
South Australia 5042, Australia

Sunil Kumar and Hans J. Griesser
Ian Wark Research Institute, University of South Australia, Mawson Lakes, Adelaide,
South Australia 5095, Australia

The localized availability of bioactive biomolecules directly at the implant/tissue interface presents a promising strategy for improved wound healing and thus biointegration. Bioactive molecules that cannot be incorporated into the bulk material of a device may be delivered from a compatible surface coating, while the reservoir capacity of thin surface coatings is limited, they offer localized delivery over the first few critical hours or days of wound healing. In this study an alginate/chitosan hydrogel has been utilized as the basis for nanoscale eluting coatings to provide a hydrophilic yet water insoluble surface delivery system. The release characteristics of these hydrogel coatings were measured by employing the model molecules-fluorescein isothiocyanate dextran [FD; molecular weights (MWs) 4, 70, and 2000 kDa], fluorescein isothiocyanate albumin, and rhodamine. Scanning electron microscopy and atomic force microscopy were used to study the morphology of the hydrogel coatings on model substrates, and ellipsometry was employed for measuring the coating thickness. On silicon wafers, the coatings were of good uniformity and conformal, with a thickness of ~120 nm and a rms roughness of 3.0 nm. A model porous substrate, paper, which afforded deep pore penetration of the hydrogel, was used to mimic hydroxyapatite. The release of FD was observed to be dependent on the MW, the release medium, charge, and surface roughness. Sustained release was recorded for FD 70 and FD 2000 with yields of about 90% and 75%, respectively, into simulated body fluid within 26 days. Concurrent elution of different molecules from one hydrogel coating was demonstrated. The observed elution profiles were fitted to release kinetics such as the Korsmeyer-Peppas model or first order release. © *2007 American Vacuum Society.* [DOI: 10.1116/1.2751126]

I. INTRODUCTION

The surface composition and associated properties are key determinants for the successful integration of implants into biological tissues. A central strategy in the development of biomedical devices is to create biomimetic surfaces for directing the natural biological response.[1] Toward this aim, one strategy is the local delivery of specific biologically active molecules such as extracellular matrix adhesion proteins, growth factors, cytokines, and antibacterials, directly at the implant/tissue interface in order to elicit predictable, targeted local host responses.[2] Many bioactive molecules, however, cannot be incorporated and delivered from many of the commonly used biomaterials used to fabricate devices. In such cases, bioactive molecules must be delivered from a surface coating that needs to meet a number of other criteria. The loading capacity of surface coatings is, of course, limited, but may suffice to deliver bioactive molecules during the initial, most active stage of integration of implants with a host.

In comparison with bulk delivery systems, surface delivery by eluting coatings is advantageous in enabling independent selection of the implant bulk material to satisfy other criteria. In addition, an eluting coating can be developed on a well-defined model surface for fundamental studies. Furthermore, micropatterning, for example, by combining plasma treatment and lithography, can be used to study interfacial interactions (e.g., mechanisms of bioadhesion).[3] The deployment of drug eluting coatings on established metallic, ceramic, or polymeric endoprosthetic biomaterials has great potential for widespread use.[2,4] Various eluting coatings have been designed on the basis of current understanding of the biology and biochemistry of cellular function and differentiation.[2,5–10]

Site-specific surface delivery strategies are of considerable interest[11,12] for drug release at the surface of devices such as catheters, prosthetic heart valves, artificial vascular grafts, stents, and others. Among them, drug eluting stents have been most successful and have emerged in recent years

---
[a)]Author to whom correspondence should be addressed; present address: Molecular and Health Technologies, CSIRO, Bag 10, Clayton South MDC, VIC 3169, Australia; electronic mail: ping.peng@csiro.au

as a promising therapy for preventing postimplantation restenosis although the long term outcome is still in question.[13] Drugs that are antithrombotic, anti-inflammatory, and antiproliferative have been locally delivered via various polymer coatings.[14–17] In particular, sirolimus- and paclitaxel-eluting stents have been shown to be remarkably effective and have been or are undergoing extensive preclinical and clinical investigations.[18,19] However, established polymeric coatings such as PLGA may not be as suitable for the delivery of very hydrophilic bioactive molecules because of the poor solvent compatibility toward active agent, phase separation, degradation of the active species during incorporation, and so forth. Thus, there is considerable interest in the formulation of new coatings capable of local delivery[20–26] and new coating technologies.[15,27–30] Hydrogels have long been used for drug delivery and cell encapsulation[31] and appear better suited to the incorporation of proteinaceous biomolecules such as cell membrane receptor peptide ligands to stimulate target cell adhesion, spreading and growth,[32] and other hydrophilic biomolecules. Recently, the layer by layer (LBL) electrostatic assembly technique has been used for sustained delivery; LBL offers the advantage of aqueous processing.[33] However, the delivered agent was incorporated within the LBL coating as an assembly interlayer. Therefore, only biomolecules carrying a charge opposite to that of the polyelectrolyte polymer can be applied and the loading cannot be varied as electrostatic neutrality must be attained. Such a strong electrostatic interaction might also affect the biomolecule's bioactivity.

In this study we investigate alginate based hydrogels, where alginate is used as a matrix to incorporate biomolecules and as a base layer, which is then cross-linked/encapsulated by chitosan. One of the potential uses of this combination is for orthopaedic implants. Alginates are polyanionic biopolymers derived from brown marine algae and comprise 1,4-linked β-D-mannuronic and α-L-guluronic residues in varying proportions. Alginates are attractive carriers for the systemic delivery of proteins[34] and DNA (Ref. 35) and are increasingly used for cell encapsulation and tissue engineering.[36] Alginates form thin films that at low shear viscosity[37] can penetrate into the pores of porous substrates. This may provide alginate coatings both within the pores and on the surface of biomaterials such as calcium phosphate. Tuning composition, sequential structure, and molecular weight of cation-cross-linked alginate polymers provide a range of physical properties of films.[38] Alginate hydrogels appear to be well tolerated by mammalian cells and are considered suitable for adding specific biointeractions onto a "blank slate."[39] Alginate gels with a high guluronic acid content supported proliferation of rat marrow cells and their differentiation along the osteoblastic lineage.[40] A bone regeneration membrane from alginate elicited no inflammatory response[41] and new bone formation was observed inside the alginate barrier membrane at 3 weeks.[42] Ionic interactions on adding chitosan to alginate yield polyelectrolyte complexes (PECs) with enhanced and controlled mechanical properties.[43–45] A PEC can be a more effective delivery system than either alginate or chitosan alone.[46–50] Another advantage for biomedical coating applications is that water insoluble biodegradable copolymer films can be formed from aqueous solutions rather than organic solvents.[50–53]

Most uses of alginate have been in the form of beads, microbeads, block gels with other shapes, fibers, and freestanding films.[38,54] Alginate/chitosan PECs have been used as layers formed *in situ* around microcapsules, beads, and tablets or as freestanding membranes. Such layers are usually heterogeneous with a core of alginate surrounded by a PEC shell.[50,55] Only a few reports exist on alginate based coatings on solid substrates such as metal and ceramic surfaces.[56–58] Alginate has been applied to Ti and Ti alloy disks for improving bone cell adhesion on implant surfaces.[59] Our interest is different as it focuses on the use of alginate/chitosan PECs as delivery vehicles for hydrophilic molecules, in the form of thin film coatings on solid substrates. We have applied such films to model substrates and measured the release of hydrophilic, fluorescent model molecules of varying molecular weights, and charge.

II. MATERIALS AND METHODS

A. Materials

Sodium alginate, chitosan (minimum 85% deacetylated), fluorescein isothiocyanate labeled dextran with molecular weights of 4300, 71 600, and 2 000 000 Da (FD 4, FD 70, and FD 2000), rhodamine B, and fluorescein isothiocyanate labeled albumin (FITC-albumin) (all from Sigma-Aldrich) were used as received. These model release molecules were dissolved into 2.2% sodium alginate aqueous solution and the resultant solution was used for casting coatings, with a dried weight ratio of 1:12 (molecule/alginate) unless otherwise stated.

Cellulose nitrate filter paper (0.45 μm, Sartorius, Germany) was used as a porous model substrate and silicon wafers (orientation, [100]; type, P/boron doped, one side polished; thickness, 475–575 μm, Micro Materials & Research Consultancy Pty. Ltd., Australia) as smooth nonporous substrates for the application of alginate based coatings.

B. Alginate/chitosan coatings on porous model substrates (filter paper)

Filter paper coupons of 1 cm^2 area were fixed onto a glass substrate of the same size by double-sided sticky tape. 0.2 ml sodium alginate solution loaded with fluorescent molecules was applied such as to fully cover the filter paper, followed by spinning at a rate of 5500 rpm for 7 s unless otherwise stated. After drying at room temperature, the coated sample was immersed in 1M CaCl$_2$ for 3 min (for cross-linking to occur). It was then transferred to 30 ml of Milli-Q water. After blotting off excess water, the sample was left to dry. Next, it was soaked in 0.5% chitosan solution for 9 min, followed by dipping twice in 30 ml Milli-Q water. After drying again at room temperature ($\sim$10 min) to constant weight, samples were stored in clean polystyrene containers at 4 °C for ten days, sealed with Al foil.

C. Alginate/chitosan coatings on smooth substrates (silicon wafer)

Silicon wafers were cut to 7×12 mm^2 size and washed in acetone, rinsed with Milli-Q water, and soaked in 5% NaOH for 5 min. After dipping in Milli-Q water, they were immersed in $2M$ HCl solution for 1 min, then rinsed with Milli-Q water, and dried under a stream of filtered compressed air for immediate use. Wafers were initially spin coated with 20 μl of a 0.25% chitosan solution at a speed of 5500 rpm for 9 s, which was quickly dried while the spinning continued and then allowed to stand in air for another 2 min. Application of this initial chitosan layer as adhesion promoting layer for the alginate film improved the application and uniformity of the subsequent alginate coating. Alginate coatings were then applied in the same way as for filter paper except that 100 μl of alginate solution was used. A chitosan solution was then spin coated onto the dried alginate layer, spotting 100 μl of a 0.5% chitosan solution onto the sample and incubating for 9 min before spinning the sample at 5500 rpm for 9 s. The remainder of the procedure was the same as that on paper substrates.

In order to investigate the possibility of concurrent localized delivery of multiple compounds, rhodamine B and FD70 were dissolved into the same alginate solution and used for coatings on silicon wafers cast in the same way as above.

D. Alginate/chitosan coatings on gold coated quartz crystal microbalance (QCM) crystal substrates

A gold coated 10 MHz QCM crystal [International Crystal Manufacturing (ICM), Oklahoma, OK] was cleaned by an air plasma (Plasma cleaner/sterilizer, PDC-32G, Harrick Scientific Corporation) for 2 min and then rinsed with anhydrous ethanol. Next, a self-assembled monolayer (SAM) of 11-mercaptoundecanoic acid was adsorbed onto the gold surface of the crystals from a 10 mM solution in ethanol for 3 h. The sample was rinsed with water and dried with a stream of filtered air for immediate use. The carboxylic acid SAM served as an adhesion promoting layer for the subsequent chitosan films. The preparation of alginate/chitosan coatings on Au/SAM/chitosan coated quartz crystal substrates followed the same procedures as for alginate/chitosan coatings on silicon wafer substrates, except for spinning the coatings at 4000 rpm for 6 s for both alginate and chitosan solutions.

E. Morphology and thickness analysis

The morphology of hydrogel coatings on paper and Si wafers was examined by field emission scanning electron microscopy (SEM, Philips XL30) at an acceleration voltage of 5–10 kV. Samples were carbon coated prior to analysis. Atomic force microscopy (AFM) (Digital Instruments Nanoscope III Multimode microscope) images were recorded in tapping mode under ambient conditions in air using an etched silicon probe (model TESP). Image processing was conducted using Nanoscope Version 4.43b26. Surface rough-

ness was calculated as root mean square (rms) values derived from the AFM image analysis. The thickness of dehydrated films was measured with a Beaglehole ellipsometer by analysis at ten different incident angles on the sample, using a wavelength of 600 nm, a refractive index of silicon wafer of 3.95,[60] and assuming an initial refractive index of the film of 1.53.[61]

F. QCM experiments

The coated crystal was mounted into a cell holder (1 CM Lever Oscillator). The assembly was put into a Faraday cage (EQCN-702, ELCHEMA). The resonance frequency was measured using a Universal counter (53131A, 225 MHz, Agilent). The data acquisition was computer controlled and recorded via Excel with custom designed add-ins, in time lapse mode at intervals of 2 s.

G. Release studies

Elution of the fluorescent model molecules was done from the hydrogel coatings into the following media.

1. Phosphate buffered saline (PBS, pH 7.4).
2. Simulated body fluid (SBF). 1.67 mM of K_2HPO_4, 2.5 mM of $CaCl_2$, and 137.8 mM of NaCl dissolved in Milli-Q water and pH adjusted to 7.2 by addition of 50 mM of tris(hydroxymethyl)aminomethane $[(CH_2OH)_3CNH_2]$ and $1M$ hydrochloric acid.
3. Mixture of SBF and PBS. The pH of SBF was adjusted to 7.4 with $0.01M$ NaOH and then mixed with PBS at different PBS:SBF ratios of 2:1, 1:1, and 1:2.

A luminescence spectrometer (Perkin-Elmer LS 55) was used to measure the fluorescence of the molecules eluted into the aqueous media (3 ml) at 37 °C with slow stirring. The fluorescence intensity was measured using wavelengths for excitation and emission of 490 and 517 nm, respectively, for FITC-dextran, 490 and 512 nm for FITC-albumin, and 555 and 610 nm for rhodamine, all at a slit width of 5 nm, in time lapse mode. To obtain the percentage of embedded fluorescent molecules and thus the total release (100%), parallel samples were produced without allowing further crosslinking by dehydration, by immersing samples immediately after spin coating into 3 ml PBS (pH=7.4) for FITC-dextrans and rhodamine or 3 ml PBS (pH=10, adjusted with $1M$ NaOH) for FITC-albumin and measuring the fluorescence after 7 day elution at 4 °C. The sample size for release studies was 7×12 mm^2 for Si wafers and 3×3 mm^2 for the paper substrates.

Elution data (release percentage versus time) models were tested based on linear regression analysis,[62] linearizing nonlinear models where appropriate. Analysis of Variance (ANOVA) was used to test the statistical significance of release models to the significant value of the F statistic at a level of 0.05. If the value of F is less than 0.05, then the data sets fitted well to a linearized model. Furthermore, the strength of the relationship between the model and experi-
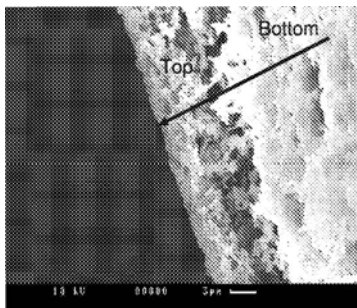
FIG. 1. Cross-section SEM micrograph of a sample comprising a coating of alginate/chitosan blend hydrogel on paper substrate.
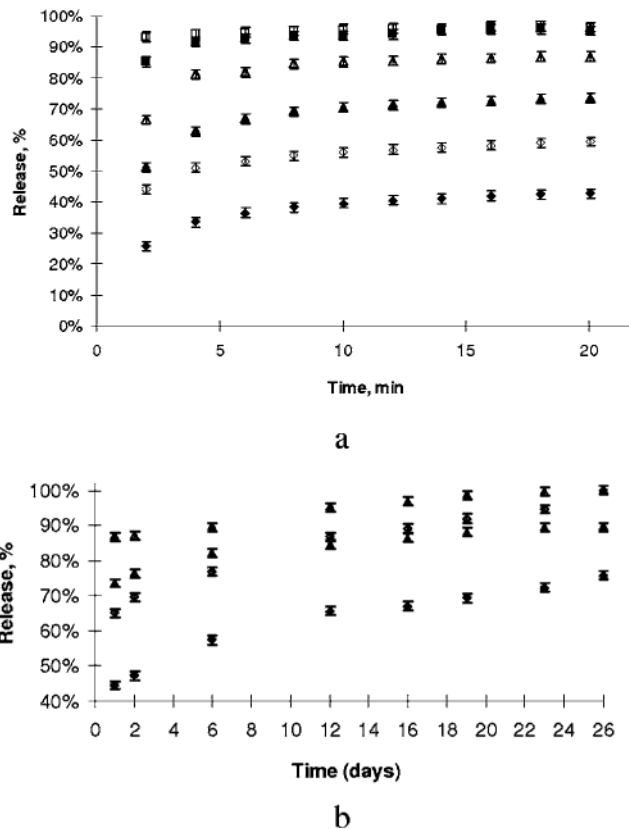

FIG. 2. (a) Release of FITC-labeled dextrans from alginate/chitosan coatings on paper substrate, over the first 20 min. (b) Release of FITC labeled dextrans from alginate/chitosan coatings on paper substrate over 26 days. FD4 (SBF), ■; FD4 (PBS), □; FD70 (SBF), ▲; FD70 (PBS), △; FD2000(SBF), ◆; FD2000(PBS), ◇.

mental release profile was assessed via the multiple correlation coefficient[63] R, where a large value indicates a strong relationship.

The Jonckheere-Terstra test was chosen to compare release profiles where exact tests were selected to calculate statistical significance levels by the Crosstabs and nonparametric test procedures.[62] The nonparametric test makes no assumptions about the distribution of the data; thus, significance can be assessed even when the data fail to meet underlying assumptions necessary for statistically reliable results using a standard asymptotic method. If the value of exact significance is less than 0.05, there is a significant difference among the compared data sets.

III. RESULTS AND DISCUSSION

AFM images (not shown) of alginate/chitosan coatings on silicon wafers showed smooth and homogeneous surfaces, with rms values of ~3.0 nm.[64] The thickness of the dehydrated coatings was measured to be ~120 nm by ellipsometry,[64] and the same value was obtained by cross-section SEM (Ref. 64) (not shown).

SEM analysis also showed that the alginate/chitosan coatings on paper maintained the original morphology of the porous structure of the substrate surface, which implies that it is possible to maintain designed morphology of substrates such as hydroxyapatite-sprayed orthopaedic implants.[64] In addition, cross-section SEM images revealed that alginate/chitosan coatings penetrated into the pores of porous substrates (Fig. 1), indicating the possibility to utilize the pores of hydroxyapatite coatings as reservoirs for release from alginate coatings.

Alginate/chitosan bulk hydrogels are well known to be highly swellable when soaked in water.[65] QCM study of alginate/chitosan coatings on gold coated quartz crystals showed adsorption of various amounts of water depending on environmental humidity. Saturated humidified air caused a decrease of the frequency, whereas the frequency signal was stable in a dry air environment.

A. Effect of release medium on release behavior

The medium was found to have a marked influence on the release profiles from the paper substrate. The release percentage was lower in SBF than in PBS for all molecular weights

(MWs) of incorporated FD, as shown in Fig. 2(a). The difference in elution into the two media was more pronounced for the larger MW FD. Within 20 min, the released amount was 73.5% and 42.7% for FD 70 and FD 2000, respectively, in SBF, whereas the corresponding yields reached 86.9% and 59.5% in PBS, respectively. Following initial fast release of a substantial fraction of the loading, sustained slower release was observed for FD 70 and FD 2000 in both media for up to 26 days [Fig. 2(b)]. When eluting into SBF, residual amounts of 25% for FD 2000 and 10% for FD 70 remained in the coatings, whereas FD of both MWs was eluted to almost 100% into PBS. Moreover, a significant decrease also resulted in the released percentages when decreasing the ratio of PBS in PBS/SBF mixtures (Fig. 3). As the total ionic strength was maintained and the pH difference of the two release media is only 0.2 u, Ca^{2+} ions are thus considered to be the major cause of the decreased elution efficiency into SBF. In addition to osmotic pressure between the hydrogel and SBF at the initial incubation phase, Ca^{2+} ions can diffuse into the interstices of the alginate/chitosan coacervate and bind to residual carboxylic groups, further cross-linking the gel films and thereby reducing the elution of our probe molecules. This interpretation is consistent with the observation of lower permeability to water when $CaCl_2$ was added to alginate/chitosan PEC membranes.[50] When the percentage of
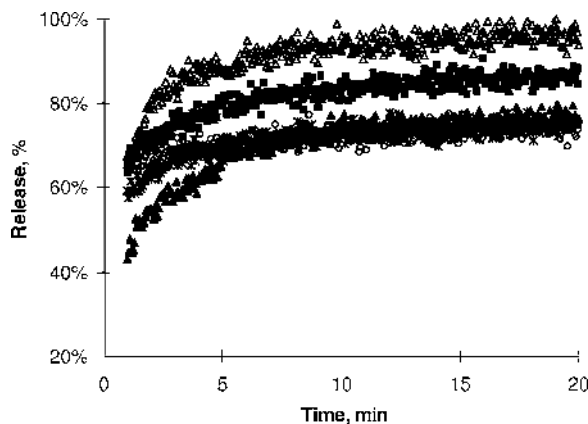
FIG. 3. Effect of the ratio of PBS to SBF on the release of FD 70 from alginate/chitosan coatings, on paper substrate. Ratios of PBS to SBF are 3:0 (△), 2:1 (■), 1.5:1.5 (▲), 1:2 (○), and 0:3 (×).

SBF was in the range of 0%–50%, the effect due to Ca^{2+} increased with concentration (Fig. 3). On further increasing the percentage of SBF from 50% to 100%, the release remained almost constant with significance (two-tailed) of 0.37 by the Jonckheere-Terpstra test, suggesting that the alginate/chitosan coatings were saturated with Ca^{2+} ions at 50% or higher SBF content in the eluting medium.
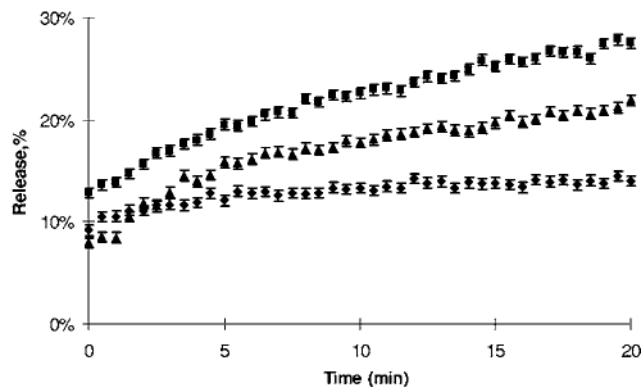
B. Effect of molecular weight on release of FD

For comparison with the paper substrates, coated silicon wafers were also used in this study. Figure 4 shows that the release of FD was MW dependent, as expected for diffusion controlled release. The release rate was much faster over the first few hours but sustained release could be detected for 3 days for FD 70 and FD 2000 and for 2 days for FD 4 with silicon wafer substrates in SBF.

We considered whether the release might be due mainly to dissolution of the alginate/chitosan PEC coating. Interference fringes (arising from the presence of the thin film on the Si wafer substrate) were, however, still clearly visible after 3 days (Ref. 64) (data not shown), indicating that the coating had not thinned appreciably. In addition, we performed photobleaching of the remaining FD in the coating (data not shown), and this confirmed qualitatively that some FD (and some coating) was still present for FD 70 and FD 2000.

For all MWs, over a given time interval a lower release percentage was observed with FD loaded alginate/chitosan coatings on silicon wafers compared with the same coatings on paper substrates. This may be a reflection of the topography of the coatings.

The total amount of FD released into 3 ml SBF from coatings on paper was higher than for coatings on silicon wafers despite a smaller sample size (0.84 cm^2 for silicon wafers and 1 cm^2 for paper substrates) (Table I). This is attributed to the hydrogel filling the pores of the paper substrate as well as coating its surface. Therefore, more sustained release for FD 70 and FD 2000 on the paper substrates was detected with yields of about 90% and 75%, respectively, over 26 days.

a
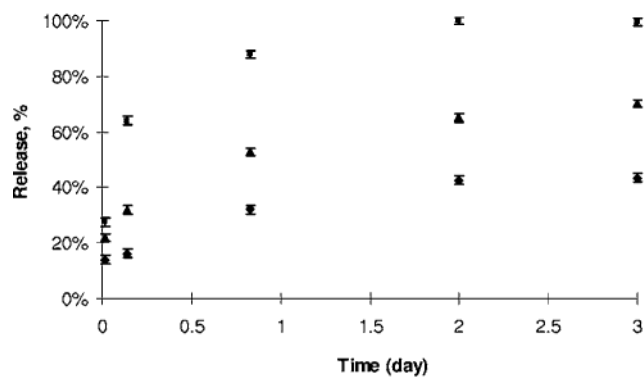
b

FIG. 4. Effect of molecular weight on the release of fluorescently labeled dextrans from alginate/chitosan coatings on silicon wafers into SBF medium, (a) over 20 min; (b) over 3 days. 4 kDa, ■; 70 kDa, ◇; 2000 kDa, ●.

C. Release kinetics

For the alginate/chitosan hydrogel coatings with a thickness of ~120 nm on silicon wafers, the release system can be considered as a slab/monolithic model[66] since the width (7 mm) and the length (12 mm) of the sample far exceed the coating thickness. In this case we need to consider the two factors of diffusion of the solute and the swelling of the hydrogel layer in the aqueous solution.[67,68] Swelling will, of course, affect the diffusion rate of the solute and the thickness of the layer the solute needs to diffuse through.

For the release data obtained within the initial 20 min of elution, dual phase kinetics was used to fit the experimental

TABLE I. Total amount of released FITC-dextran in SBF.

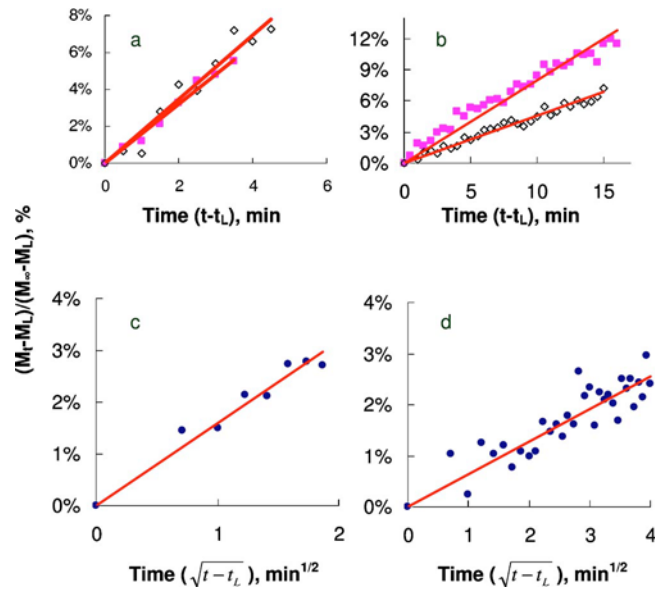| Substrate	Accumulated release concentration in 3 ml in ppb	
	Silicon wafer	Paper
Total days	3	26
FD 4	82	⋯
FD 70	84	372
FD 2000	26	272

FIG. 5. Release kinetics from alginate/chitosan coatings on silicon wafers into SBF over 20 min. (a) Zero order release kinetics for FD 70 (○) and FD 4 (●) within the first few minutes; (b) Zero order release kinetics for FD 70 (○) and FD 4 (●) after the first few minutes; (c) Diffusional release kinetics for FD 2000 within the first few minutes; (d) Diffusional release kinetics for FD 2000 after the first few minutes.

data according to the Korsmeyer-Peppas model.[66,68] As shown in Fig. 5(a), burst release was observed at the very beginning, at $t < 4$ min for FD 4 and < 5 min for FD 70, where the following linear expression (zero order)[66] displayed a good fit as summarized in Table II.

$$\frac{(M_t - M_L)}{(M_\infty - M_L)} = k(t - t_L), \tag{1}$$

where M_t is the released amount at time t, M_∞ is the total loaded amount, M_L is the released amount at time t_L when the zero order release begins, and k is a release constant.

After the initial burst release period, the release of both FD 4 and FD 70 can also be fitted to a linear expression (zero order) but with significantly lower release rates as indicated

by the smaller slopes [Fig. 5(b)]. The ANOVA test showed that the significant value of the F statistic at a level of 0.05 for the regression was zero.

The burst release was not as pronounced for FD 2000 but its elution within the first 3.5 min was nevertheless faster than over the subsequent time interval up to 20 min. The initial release was better described by the following equation[66] after 0.5 min [Fig. 5(c)]:

$$\frac{(M_t - M_L)}{(M_\infty - M_L)} = k(t - t_L)^{0.5}. \tag{2}$$

ANOVA test showed that the significant value of the F statistic at a level of 0.05 for the fitting was zero. The subsequent release after the initial few minutes was also better described by Eq. (2) than by Eq. (1) but the linear curve [Fig. 5(d)] had a smaller slope as compared to Fig. 5(c).

In the initial burst release stage, the release rate was almost the same for FD 4 and FD 70 [Fig. 5(a)], despite the difference in MW, whereas afterwards the release rate varied inversely with MW [Fig. 5(b) and 5(c)]. This behavior can be explained by considering both the swelling of the hydrogel and the difference in the diffusion coefficient or mobility of FDs of different MWs incorporated to the same weight ratio of alginate to FD. During the process of hydrogel coating preparation, the loaded FD was originally dissolved in alginate polymer solution. As the water evaporated, a glassy alginate/chitosan matrix resulted,[47,67,70] with FD dispersed in it. The matrix has the morphology of a hydrogel that is nonporous[67] but molecularly permeable. Upon soaking in the aqueous release medium, the hydrogel polymer matrix swells and the glass transition temperature of alginate is lowered,[71] water uptake produces a rapid change to a new equilibrium volume[72] and the swelling hydrogel polymer matrix transforms into the rubbery state. Polymer matrix relaxation dominates the initial burst release,[68] and fast, zero order burst release of FD 4 and FD 70 is thus observed. As FD 70 has a smaller diffusion coefficient than FD 4, FD 70 displayed a slower release, as shown in Fig. 5(b). However, in the very early few minutes, desorption of FD from the outer surface of the hydrogel may also play a role in the burst

TABLE II. ANOVA analysis of release model fit for the release of FD 4 (before 4 min) and FD 70 (before 5 min) on Si wafer in SBF.

Predictor	Dependent variable	Regression coefficient k		R		R square	
		FD 4	FD 70	FD 4	FD 70	FD 4	FD 70
t-t_L	$\frac{(M_t - M_L)}{(M_\infty - M_L)}$	0.016	0.017	0.997	0.991	0.995	0.982
Source of variance	Sum of squares			df		Mean square		F[a]	
		FD 4	FD 70	FD 4	FD 70	FD 4	FD 70	FD 4	FD 70
Regression		0.009	0.021	1	1	0.009	0.021	Value	1344.153	487.574
Residual		0.000	0.000	7	9	0.000	0.000	Sig.	0.000	0.000
Total		0.009	0.022	8	10					

[a]At the 0.05 level.

release, which is less dependent on the molecular weight than diffusion from within the hydrogel layers, as indicated in Fig. 5(a). In contrast, the larger FD 2000 has a substantially smaller molecular diffusion constant; its rate of diffusion is less dependent on the matrix swelling, and thus FD 2000 diffuses comparatively much more slowly through and out of the alginate/chitosan gel, without a substantial initial burst release. The release of FD 2000 is proportional to the square root of the release time and appears to be controlled by diffusion in the alginate/chitosan hydrogel layer.

The swelling of the alginate/chitosan matrix may also enable configurational rearrangement motions that lead to closer alignment of molecular chains and oppositely charged groups in the PEC matrix[50] and hence densification through the formation of additional cross-links.[70] On the other hand, as discussed before, Ca^{2+} ions can also further cross-link the gel films at pH 7.2, which act as either a complement or a competitor to the PEC formation. More extensive chain alignment and pairing of oppositely charged groups would reduce the translational and rotational mobilities of hydrogel polymer chain segments and thereby reduce the diffusion coefficients of FDs. Such time dependent changes (both swelling and chain rearrangements) to the matrix structure would also be expected to make the release kinetics more complex than for simple polymeric delivery systems. A further effect that needs to be considered is the considerable polydispersity of the FD compounds. The diffusion coefficient is inversely proportional to the cubic root of the molecular weight.[73] As the larger size fractions diffuse more slowly, this also contributes to release kinetics that does not match closely a simple model. Thus it is not surprising that the FD/alginate/chitosan systems show both fast burst release and extended, ever slowing elution.

The release of FD of MWs 4 and 70 kDa from alginate/chitosan hydrogels within the first 20 min appears to correspond to Case II transport,[66,69,72] or non-Fickian transport, with the rate practically independent of time under the two different time segments, while diffusion[66,69,72] appears to be the main mechanism for the release of larger molecules such as FD 2000.

At longer times, between 20 min and 3 days, the release data [Fig. 4(b)] were best fitted to first order kinetics[74]

$$\frac{(M_\infty - M_t)}{(M_\infty - M_f)} = e^{-k(t-t_f)} \qquad (3)$$

or

$$Ln\frac{(M_\infty - M_t)}{(M_\infty - M_f)} = -k(t-t_f), \qquad (4)$$

where M_t and M_∞ are the released amount, at time t and the overall released amount, respectively, M_f is the released amount at time t_f when the first order release model begins, and k is the release constant.

The plot of $\ln[(M_\infty - M_t)/(M_\infty - M_f)]$ vs $(t-t_f)$ yields approximately linear relationships (Fig. 6) although there is a systematic deviation from linearity, suggesting again a diffusion rate that decreases over time. In addition, the first order
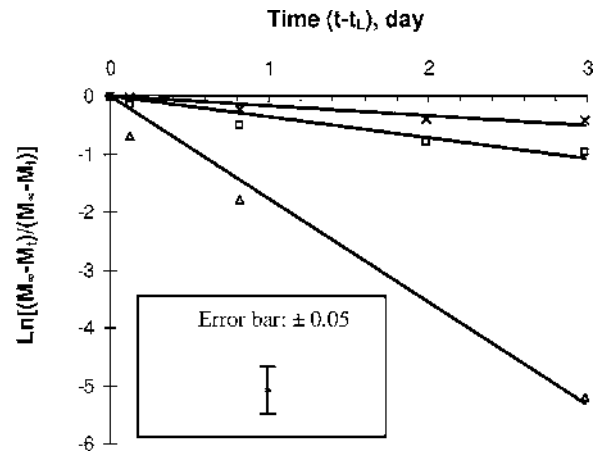

FIG. 6. Approximate first order release kinetics of blend hydrogel coatings on silicon wafers up to 3 days. 4 kDa ($\triangle$), 70 kDa ($\square$), and 2000 kDa (X).

constant decreases with increasing MW of the loaded FD molecules. In this time period it is reasonable to assume that the hydrogel has swelled and rearranged to equilibrium, and release proceeds in the customary concentration-dependent first order manner, with superimposed effects from polydispersity causing deviation.

D. Effect of thickness of hydrogel coatings on release

Different thicknesses of alginate/chitosan hydrogel coatings on silicon wafers were obtained by varying the spinning time while casting 2.2% aqueous alginate solution, also containing FD 70 at a weight ratio of 12:1 (alginate:FD). By ellipsometry the thickness of the dehydrated coatings was determined to be 215, 120, and 110 nm, when using spinning times of 3, 7, and 9 s, respectively. As shown in Fig. 7(a), the released percentage over a given time period decreased with increasing coating thickness. A comparison of the slopes of the release curves indicates that the thicker coatings led to a somewhat reduced release rate.

As 2.2% aqueous alginate solution containing FD 70 at a weight ratio of 12:1 is stable during storage without observable phase separation, we presume that the concentration of FD 70 within the coating is constant for each sample regardless of different thicknesses. Accordingly, the slower but more sustained release at increased thickness can be assigned to a higher loading of FD 70 and increased diffusional distances as the coating thickness increases.

E. Effect of the FD 70 content on release

Coatings were prepared on silicon wafers with alginate/FD 70 weight ratios of 12:1, 8:1, and 5:1 and elution experiments conducted into SBF at 37 °C. The greater the content of alginate, the slower was the release of FD 70 from hydrogel coatings [Fig. 7(b)]. The burst release within the initial ~5 min was more pronounced with increased loading of FD, which causes a larger driving force by the gradient of the chemical potential. In addition, the diffusion coefficient of FD 70 increases as the gel becomes less dense with re-
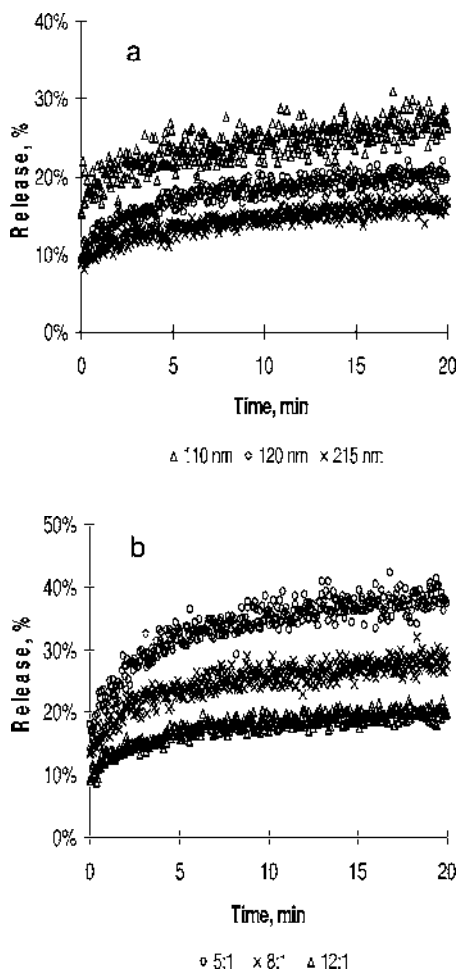
FIG. 7. Effect of thickness of alginate/chitosan coatings (a) and effect of the ratio of alginate to FD 70 in alginate/chitosan coatings (b), on silicon wafers, on the release of FD 70 into SBF.
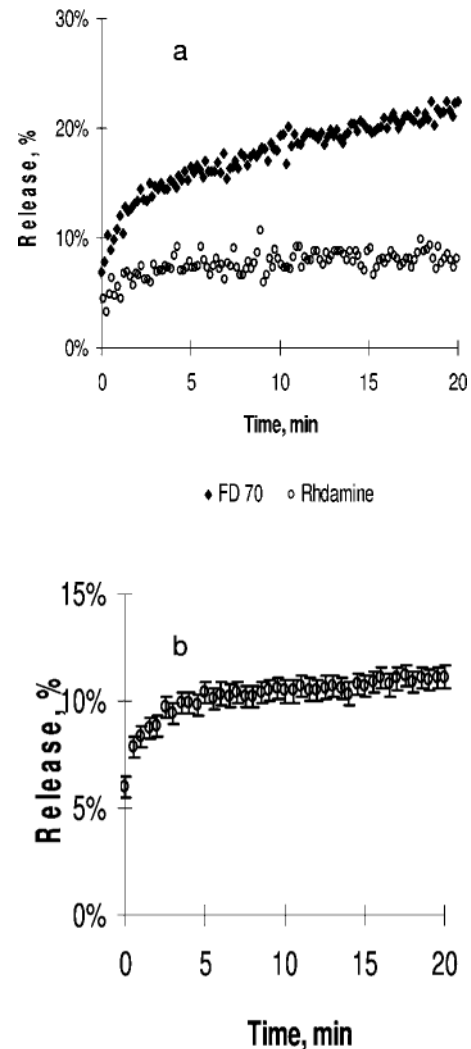

FIG. 8. Concurrent release of FITC-dextran and rhodamine (a) and slower release of FITC labeled albumin (b) from alginate/chitosan coatings on silicon wafer into SBF.

duced alginate content. The same phenomenon was observed in the release of FITC labeled bovine serum albumin from alginate/chitosan microspheres.[49] After the initial burst release, however, the release was little affected by the loading and presented a good linear relationship with time. ANOVA test of the linear model showed that the significant value of the F statistic at a level of 0.05 for the regression was zero.

F. Concurrent release and electrostatic effects of loaded molecules on release

Alginate/chitosan coatings loaded simultaneously with rhodamine B and FD 70 on silicon wafers showed that both solutes can be released concurrently from a hydrogel coating [Fig. 8(a)]. Rhodamine demonstrated a much slower release rate despite its smaller MW (479 Da). This can be assigned to the presence of attractive electrostatic interactions between the protonated amine group of rhodamine B and carboxyl groups of alginate.

When loading albumin into an alginate/chitosan PEC coating, however, the release of albumin was slower than that of FD 70 [Fig. 8(b)]. With a MW of albumin of 66 kDa,

the MW is comparable. Albumin is net negatively charged (pI=4.8) in alginate (at pH 6.91), but perhaps local charge effects in such a heterogeneous protein molecule are more important. Positively charged (protonated) Lys and Arg amino acid residue in albumin can interact electrostatically with carboxyl groups in alginate. The local structure of a protein might play an important role in its elution from charged PEC matrices and the isoelectric point may not be a reliable predictor. On the other hand, the possibility also exists that carboxylate groups interact with chitosan, again causing electrostatic attraction and consequent slowing of diffusional transport. The diffusion of molecules with various charged groups through polyelectrolyte complex hydrogels may be affected by multiple factors.

IV. CONCLUSIONS

An alginate/chitosan polyelectrolyte complex can serve as a thin surface coating on substrates that provides a hydrophilic yet water insoluble release matrix for hydrophilic mol-

release, which is less dependent on the molecular weight than diffusion from within the hydrogel layers, as indicated in Fig. 5(a). In contrast, the larger FD 2000 has a substantially smaller molecular diffusion constant; its rate of diffusion is less dependent on the matrix swelling, and thus FD 2000 diffuses comparatively much more slowly through and out of the alginate/chitosan gel, without a substantial initial burst release. The release of FD 2000 is proportional to the square root of the release time and appears to be controlled by diffusion in the alginate/chitosan hydrogel layer.

The swelling of the alginate/chitosan matrix may also enable configurational rearrangement motions that lead to closer alignment of molecular chains and oppositely charged groups in the PEC matrix[50] and hence densification through the formation of additional cross-links.[70] On the other hand, as discussed before, Ca^{2+} ions can also further cross-link the gel films at pH 7.2, which act as either a complement or a competitor to the PEC formation. More extensive chain alignment and pairing of oppositely charged groups would reduce the translational and rotational mobilities of hydrogel polymer chain segments and thereby reduce the diffusion coefficients of FDs. Such time dependent changes (both swelling and chain rearrangements) to the matrix structure would also be expected to make the release kinetics more complex than for simple polymeric delivery systems. A further effect that needs to be considered is the considerable polydispersity of the FD compounds. The diffusion coefficient is inversely proportional to the cubic root of the molecular weight.[73] As the larger size fractions diffuse more slowly, this also contributes to release kinetics that does not match closely a simple model. Thus it is not surprising that the FD/alginate/chitosan systems show both fast burst release and extended, ever slowing elution.

The release of FD of MWs 4 and 70 kDa from alginate/chitosan hydrogels within the first 20 min appears to correspond to Case II transport,[66,69,72] or non-Fickian transport, with the rate practically independent of time under the two different time segments, while diffusion[66,69,72] appears to be the main mechanism for the release of larger molecules such as FD 2000.

At longer times, between 20 min and 3 days, the release data [Fig. 4(b)] were best fitted to first order kinetics[74]

$$\frac{(M_\infty - M_t)}{(M_\infty - M_f)} = e^{-k(t-t_f)} \tag{3}$$

or

$$Ln\frac{(M_\infty - M_t)}{(M_\infty - M_f)} = -k(t - t_f), \tag{4}$$

where M_t and M_∞ are the released amount, at time t and the overall released amount, respectively, M_f is the released amount at time t_f when the first order release model begins, and k is the release constant.

The plot of $\ln[(M_\infty - M_t)/(M_\infty - M_f)]$ vs $(t-t_f)$ yields approximately linear relationships (Fig. 6) although there is a systematic deviation from linearity, suggesting again a diffusion rate that decreases over time. In addition, the first order
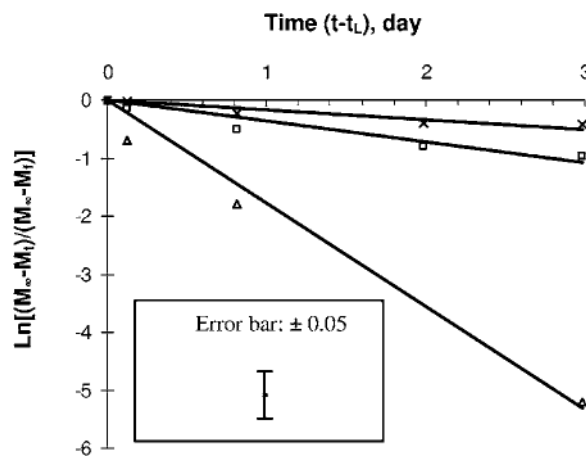

FIG. 6. Approximate first order release kinetics of blend hydrogel coatings on silicon wafers up to 3 days. 4 kDa (△), 70 kDa (□), and 2000 kDa (X).

constant decreases with increasing MW of the loaded FD molecules. In this time period it is reasonable to assume that the hydrogel has swelled and rearranged to equilibrium, and release proceeds in the customary concentration-dependent first order manner, with superimposed effects from polydispersity causing deviation.

D. Effect of thickness of hydrogel coatings on release

Different thicknesses of alginate/chitosan hydrogel coatings on silicon wafers were obtained by varying the spinning time while casting 2.2% aqueous alginate solution, also containing FD 70 at a weight ratio of 12:1 (alginate:FD). By ellipsometry the thickness of the dehydrated coatings was determined to be 215, 120, and 110 nm, when using spinning times of 3, 7, and 9 s, respectively. As shown in Fig. 7(a), the released percentage over a given time period decreased with increasing coating thickness. A comparison of the slopes of the release curves indicates that the thicker coatings led to a somewhat reduced release rate.

As 2.2% aqueous alginate solution containing FD 70 at a weight ratio of 12:1 is stable during storage without observable phase separation, we presume that the concentration of FD 70 within the coating is constant for each sample regardless of different thicknesses. Accordingly, the slower but more sustained release at increased thickness can be assigned to a higher loading of FD 70 and increased diffusional distances as the coating thickness increases.

E. Effect of the FD 70 content on release

Coatings were prepared on silicon wafers with alginate/FD 70 weight ratios of 12:1, 8:1, and 5:1 and elution experiments conducted into SBF at 37 °C. The greater the content of alginate, the slower was the release of FD 70 from hydrogel coatings [Fig. 7(b)]. The burst release within the initial ~5 min was more pronounced with increased loading of FD, which causes a larger driving force by the gradient of the chemical potential. In addition, the diffusion coefficient of FD 70 increases as the gel becomes less dense with re-

57, 65 (2004).

[48]L. You, Y. Zou, Q. Jing, and L. Hu, Shenyang Yaoke Daxue Xuebao1006–2858 **19**, 168 (2002).

[49]L. S. Liu, S. Q. Liu, S. Y. Ng, M. Froix, T. Ohno, and J. Heller, J. Controlled Release **43**, 65 (1997).

[50]L. Wang, E. Khor, and L.-Y. Lim, J. Pharm. Sci. **90**, 1134 (2001).

[51]A. Cardenas, W. Arguelles-Monal, F. M. Goycoolea, I. Higuera-Ciapara, and C. Penich, Macromol. Biosci. **3**, 535 (2003).

[52]F. A. Simsek-Ege, G. M. Bond, and J. Stringer, J. Biomater. Sci., Polym. Ed. **13**, 1175 (2002).

[53]L. Wang, E. Khor, A. Wee, and L. Y. Lim, J. Biomed. Mater. Res. **63**, 610 (2002).

[54]D. Seliktar and R. Beyar, WO 2005055800.

[55]F. A. Simsek-Ege, G. M. Bond, and J. Stringer, J. Appl. Polym. Sci. **88**, 346 (2003).

[56]T. Yoshioka, K. Tsuru, S. Hayakawa, and A. Osaka, Mater. Res. Soc. Symp. Proc. **734**, 333 (2002).

[57]X. Wang and H. G. Spencer, J. Appl. Polym. Sci. **61**, 827 (1996).

[58]T. Yoshioka, K. Tsuru, S. Hayakawa, and A. Osaka, Biomaterials **24**, 2889 (2003).

[59]A. Bagno, M. Genovese, A. Luchini, M. Dettin, M. T. Conconi, A. M. Menti, P. P. Parnigotto, and C. Di Bello, Biomaterials **25**, 2437 (2004).

[60]J. R. Adams and N. M. Bashara, Surf. Sci. **47**, 655 (1975).

[61]J. Voros, Biophys. J. **87**, 553 (2004).

[62]LEAD Technologies, SPPS@Base system, LEAD Technologies Inc. (2002).

[63]SPSS, Regression (2004).

[64]P. Peng, Ph.D. thesis, University of South Australia, 2005.

[65]S. J. Kim, K. J. Lee, and S. I. Kim, J. Appl. Polym. Sci. **93**, 1097 (2004).

[66]N. A. Peppas, Pharm. Acta Helv. **60**, 110 (1985).

[67]R. Langer and N. Peppas, J. Macromol. Sci., Rev. Macromol. Chem. Phys. **C23**, 61 (1983).

[68]R. W. Korsmeyer and N. A. Peppas, *Controlled Release Delivery Systems* (Dekker, New York, 1983), pp. 77–90.

[69]R. W. Korsmeyer, R. Gurny, E. M. Doelker, P. Buri, and N. A. Peppas, Int. J. Pharm. **15**, 25 (1983).

[70]C. K. Yeom and K. H. Lee, J. Appl. Polym. Sci. **67**, 949 (1998).

[71]T. Hatakeyama, K. Nakamura, and H. Hatakeyama, Kobunshi Rombunshu **53**, 795 (1996).

[72]H. L. Frisch, Polym. Eng. Sci. **20**, 2 (1980).

[73]S. F. Sun, *Physical Chemistry of Macromolecules* (Wiley, New York, 1994), pp. 236–254.

[74]P. Costa and J. M. S. Lobo, Eur. J. Pharm. Sci. **13**, 123 (2001).